10-30-2010

Compatibility of ZrN and HfN with Molten LiCl-KCl-NaCl-UCl_3

Prakash Periasamy
Boise State University

Michael F. Hurley
Boise State University

Brian M. Marx
Boise State University

Michael F. Simpson
Idaho National Laboratory

Darryl P. Butt
Boise State University

Compatibility of ZrN and HfN with Molten LiCl-KCl-NaCl-UCl_3

Prakash Periasamy
Boise State University

Michael F. Hurley
Boise State University

Brian M. Marx
Boise State University

Michael F. Simpson
Idaho National Laboratory

Darryl P. Butt
Boise State University

Abstract
The reaction kinetics of ZrN and HfN immersed in a quaternary salt of composition of 28.5% LiCl-36.3% KCl- 29.4% NaCl- 5.8% UCl_3 (in weight percent) were assessed. Coupons of ZrN and HfN were exposed to the quaternary salt at 525 to 900°C for 4 to 485 hours. The reaction kinetics of the salt-refractory interactions were assessed through physical and microstructural characterization including scanning electron microscopy, x-ray diffraction and mass spectrometry. The results indicated that ZrN and HfN lose weight under all conditions investigated. While multiple mechanisms were evident, it is proposed that dissolution and oxidation were the dominant reactions that influence the weight loss. For the overall reaction, negative apparent activation energy values of -46 and -28 kJ/mol were observed in ZrN and HfN, respectively. This seemingly anomalous activation energy was associated with the simultaneous occurrence of electrochemical dissolution and surface oxide formation.

Key Words: zirconium nitride, hafnium nitride, molten salt, negative apparent activation energy, uranium chloride, corrosion, oxidation

1. Introduction

The proposed closed fuel cycle for next generation nuclear reactors relies on the successful implementation of spent fuel separation technologies. Electrochemical processing or pyroprocessing is one of the most prominent and actively studied separation methods being considered for recycling of spent nuclear fuels [1-5]. Electrochemical processing is a batch type process in which electrorefining and subsequent cathode processing are the crucial steps. Typically, an electrorefiner consists of an anode, where the metallic spent fuel is loaded; primary and secondary cathodes, where deposition of the recovered material of interest (actinides such as uranium and plutonium) occurs; and an electrolyte made up of molten salts. An electrorefiner operates at 500°C with a controlled p_{O_2} and p_{H_2O} atmosphere [1]. Following electrorefining, the cathode (containing the deposited actinides and salt) is placed in a crucible and distilled in the cathode processor. The cathode processor operates at temperatures up to 1200°C under vacuum [6].

The operating conditions in an electrorefiner and cathode processor create an unavoidable, harsh corrosive environment for the process crucibles. However, very few systematic studies [7,8] have reported on the reaction kinetics or stability of the crucible materials under the high temperature molten salt conditions that exist during the spent fuel recycling process. Takeuchi *et al.*, [7] assessed the compatibility of different ceramic materials in simulated electrochemical reprocessing environments particular to the method developed

by the Research Institute of Atomic Reactors in Russia (RIAR). The authors proposed Si_3N_4 as the best crucible material considered. In another study, Ravi Shankar *et al.*, [8] studied plasma sprayed ZrO_2 coatings on type 316L stainless steel (SS) in molten LiCl-KCl eutectic salts under controlled argon atmosphere. Through immersion experiments carried out at 600°C for periods of up to 500 hrs, the authors found insignificant weight change on the coated 316L SS [8].

ZrN and HfN are high temperature ceramics known for their chemical inertness in extreme corrosive environments. In this study the compatibility of ZrN and HfN in contact with molten 28.5 % LiCl-36.3 % KCl- 29.4 % NaCl- 5.8 % UCl_3 (in weight percent) was assessed. Both ZrN and HfN have the same crystallographic (NaCl type) structure and similar thermodynamic properties [9,10]. Thus, the objectives of this study are to assess the compatibility of ZrN and HfN with the molten salt mixture and to investigate the reaction mechanism. Based on thermodynamic, kinetic and microstructural analysis, phenomenological models are developed to explain the possible reaction mechanism**.** With the reaction mechanism known, it is expected that this knowledge could be used to support intelligent selection of materials for containment of molten salts.

2. Experimental procedure

2.1. Materials

ZrN and HfN were hot-pressed[1] at 2000°C, from commercially available ZrN (Alfa Aaser[2], 99.5% pure, -325 mesh) and HfN (ESPI Metals[3], 99.5%pure, -325 mesh) powders.
Density measurements were done using the Archimedes method. The measured percent theoretical densities for ZrN and HfN were 97% and 94.5%, respectively. Idaho National Laboratory supplied the salt mixture that was used in this study. The salt mixture had a composition of: 28.5 % LiCl- 36.3 % KCl-29.4 % NaCl- 5.8 % UCl_3 (in weight percent). From here on, the salt will be referred to as LiCl-KCl-NaCl-UCl_3.

2.2. Molten salt immersion test

Test coupons of ZrN and HfN were cut to nominally10x5x3 mm^3 from the hot pressed plates using a low-speed diamond saw. The hot-pressed nitride plates are shown in Fig. 1. The outer grey colored layer seen in Fig. 1 was from the graphite die used in hot pressing ZrN and HfN powders. Coupons were ground to remove the outer layer till a golden color typical of ZrN and HfN was obtained. Coupons were ultrasonically cleaned for 30 minutes in acetone. The dimensions and weight of each coupon were measured and recorded before and after exposure to the molten salt mixture. The coupons and the salt were contained in a graphite boat[6]. Graphite was known to be compatible with the molten salt mixture. But graphite suffers from poor structural integrity to mechanical cleaning procedures. In this study, between successive runs, the graphite boats were replaced periodically owing to a chipping problem that occurs while mechanically cleaning of the boat after a test. Fig. 2 shows a photograph of a typical graphite boat and lid used in this study. LiCl-KCl-NaCl-UCl_3 salts are highly hygroscopic and, hence, a dry glove box purged with high purity argon gas was used for handling all materials prior to testing. The boat was sealed along the edges with a graphite lid using glue[7]. After the boat was sealed, it was transferred from the glove box to the hot-zone of the molten salt test furnace (Fig. 3). Sealing was done to prevent contact of moisture with the salt while transferring from glove box to the furnace and during initial purging of the furnace. The glue ingredients evaporate at temperatures approximately above 60°C and flushed out of the system by the flowing argon gas. A schematic drawing of the experimental setup is shown in Fig. 3.

As seen in Fig. 3, commercial grade high purity argon gas from the cylinder was flowed over a $CaCO_3$ based moisture absorber and through an oxygen-absorbing furnace filled with copper wire mesh. The gas was analyzed for moisture and O_2 using a moisture (Ametek made Model 303B) and O_2 (Ntron made Model OA1) analyzer, respectively. The exit of the furnace chamber was connected to a scrubber system (DI water) to

[1] Hot-pressing was performed at Ceramatec, 2425 South 900 West, Salt Lake City, Utah 84119, USA
[2] Alfa Aesar, 26 Parkridge Road, Ward Hill, MA 01835, USA.
[3] ESPI Metals, 1050 Benson Way, Ashland, OR 97520, USA.
[6] Graphite used was a synthetic grade pyrolitic carbon of >99.2% purity from Midwest Graphite Co., Inc., Illinois, USA.
[7] Duco cement, Trademark of Devcon.

condense any chloride salt fumes. The typical measured value of p_{O_2} and p_{H_2O} were approximately 0.01 and 2 ppm (ppm by volume), respectively. Prior to the start of the molten salt immersion test, the furnace chamber was purged with argon gas for 1 hour. After subjecting the test coupons to the immersion test, they were removed from the boat and cleaned in DI water to remove loosely bound salt particles. Following test coupon cleaning, dimension and weight measurements were recorded.

The kinetics data were expressed in weight change (Δw in mg) per unit area (cm^2), where Δw ($w_{after\ immersion\ test} - w_{before\ immersion\ test}$) is defined as the weight lost or gained during the immersion test duration. The experimental variable parameters were: (a) immersion test temperature (525, 700 and 900°C) and (b) test time (4 to 485 hrs). Virgin coupons were used for each exposure.

2.3. Characterization

After coupons were exposed to the molten salt immersion test, they were subjected to microstructural characterization using optical microscopy, scanning electron microscopy (SEM) with energy dispersive spectroscopy (EDS) using a Zeiss Supra 35VP microscope, and X-ray diffraction (XRD) using a Philips X'pert system. The salts were analyzed for elemental content using a HP 4500 inductively coupled plasma mass spectrometry (ICP-MS) before and after coupon tests, to detect any presence of dissolved reaction products.

3. Experimental results

3.1. Weight change results

Fig. 4 shows weight change as a function of time for ZrN and HfN after immersion test in molten LiCl-KCl-NaCl-UCl_3 at 525 and 700ºC. Both ZrN and HfN experienced weight loss (negative weight change values). The p_{O_2} value was maintained below 1 ppm (by volume) of O_2 for all the immersion experiments in this study. At 525ºC and for each immersion times at 4, 12 and 24 hours, the weight loss values of ZrN and HfN are approximately equal to each other (considering the error bar). At 525ºC and 96 hours ZrN exhibited around 50% more weight loss than HfN, while at lower immersion times there is negligible difference in weight loss between them. The difference in weight loss between ZrN and HfN is larger at 700ºC compared to 525ºC at all immersion times. In both the nitrides, for immersion times at 4, 12 and 24 hours, the weight loss is higher at 700ºC compared to 525ºC. However, at 96 hours the weight loss values of both the nitrides are lower at 700°C compared to 525°C.

The weight change over time at 900ºC is shown in Fig. 5. Contrary to what is seen in Fig. 4, at 900ºC the observed weight change of ZrN and HfN are similar (Fig. 5) over the reaction time range of 4 to 96 hours. In addition, the weight loss values of both the nitrides are lower at 900°C (Fig. 5) compared to 525 and 700°C (Fig. 4).

Fig. 6 shows the results of ZrN and HfN weight change at 525ºC for 485 hours (approximately 20 days, the longest reaction time in this study). ZrN exhibited around 50% more weight loss than HfN when tested for 485 hours at 525ºC.

3.2. Microstructural results

Fig. 7 shows SEM micrographs of the polished hot-pressed ZrN surface before (Fig. 7a) and after (Fig. 7b) exposure to the molten salt immersion test at 525ºC for 96 hours. The surface morphology is considerably rougher after exposure to the molten salt. The surface morphology suggests dissolution and etching of ZrN occurred. Similar surface roughening was observed in HfN as shown in Fig. 8. EDS semi-quantitative analysis was performed on the surfaces of ZrN and HfN [11]. The surface oxygen concentration (few microns thick) of as hot-pressed ZrN and HfN was 5 and 6 atom percent, respectively. After immersion test at 525ºC for 96 hours, the surface oxygen concentration of ZrN and HfN was 64 and 62 atom percent, respectively. Thus, the oxygen concentration at the surface of ZrN and HfN increased after the immersion test. The EDS results suggest the formation of an oxygen-enriched layer at the surface during reaction with the molten salt [11]. However, XRD analysis on the coupons did not show the presence of an oxide layer such as ZrO_2 or HfO_2, suggesting the oxygen was dissolved into the nitride. Although no oxide was detected, the increase in

O_2 content is likely due to the formation of a Zr-N-O type phase, as has been reported in the literature [9, 12]. The source of oxygen for this oxynitride formation is not yet clear. One of the possibilities could be the oxygen dissolved within the ZrN and HfN sintered pellets diffusing to the surface at immersion temperatures.

Coupons were cross-sectioned and polished following testing in order to analyze the reaction interface. EDS analysis revealed that the thickness of the oxygen-enriched layer increased with either reaction temperature or time. Table 1 shows the thickness of oxygen-enriched layer for ZrN. In ZrN tested for 96 hours, the thickness of the oxygen-enriched layer increased from 30 to 70 μm with increase in reaction temperature from 525 to 900°C. A similar trend was observed in HfN also.

3.3. XRD results

In a separate experiment, ZrN powders were mixed with LiCl-KCl-NaCl-UCl_3 and reacted at 900ºC for 1 hour with p_{O_2}value less than 1 ppm (ppm by volume). After the test, the solidified mixture was crushed into powders and XRD was performed. The main objective of this experiment was to increase the surface area for the reaction and to identify any reaction products that go undetected when analyzing the bulk nitrides. Fig. 9 shows the resulting XRD spectrum, which identifies UO_2 as a new phase (instead of UCl_3) among other reactant compounds. Similar results were observed in ZrN powders reacted with the salt at 900ºC for 4 hours.

3.4. ICP-MS results

ICP-MS analysis was performed to analyze the presence of Zr and Hf ions in LiCl-KCl-NaCl-UCl_3 salt before and after immersion experiments. Zr and Hf ions in the LiCl-KCl-NaCl-UCl_3 salt prior to immersion experiments (i.e., in as-received condition) were less than 1 atomic ppm. LiCl-KCl-NaCl-UCl_3 salts were collected from the graphite boat after the immersion experiments at 525, 700 and 900°C for 96 hours in which ZrN was reacted with LiCl-KCl-NaCl-UCl_3. Table 1 shows the ICP-MS result together with the corresponding weight change and thickness of the oxygen enriched layer for each immersion experiment. After immersion experiment at 525 and 700°C for 96 hours, the Zr ion concentrations present in the salt were 204 and 82.1 appm (atomic parts per million), respectively. Results clearly indicate the increase of Zr ion concentration in LiCl-KCl-NaCl-UCl_3 after the immersion experiment. Concentration of Zr ions decreased as the reaction temperature increased from 525 to 700°C.

4. Discussion

As illustrated in Figs. 4-6, ZrN and HfN experienced weight loss when exposed to the molten salt mixture between 525 and 900°C. High temperature molten salt compatibility studies with other materials systems such as SiC [13] and Al_2O_3 [14] are well documented. Bourg *et al.* [15] studied the reaction of ZrN under Cl_2 gas and LiCl-KCl eutectic mixture at 500°C. The weight loss observed in this study [15] was attributed to (i) the formation of volatile reaction products and/or (ii) electrochemical dissolution. Hence, based on previous observations [15], it is of interest to consider candidate electrochemical processes and formation of any volatile reaction products such as chlorides to explain weight loss observed in ZrN and HfN.

4.1. Thermodynamics of reactions of ZrN and HfN with LiCl-KCl-NaCl-UCl_3

ZrN and HfN can react to form Zr-Cl and Hf-Cl gaseous products (Fig. 10), respectively, provided there is sufficient concentration of chlorine. Thermodynamic calculations in Fig. 10 were performed using HSC Outokompu software. Fig. 10 indicates that amongst the Zr-Cl and Hf-Cl compounds, $ZrCl_4$ and $HfCl_4$ are favored volatile compounds, since they posses the most negative free energy among likely constituents. In this study, Cl_2 was not introduced directly as in the case of Bourg *et al.* [15]. The possible sources of free Cl_2 or Cl^- ions in this study are discussed later.

4.2 Uranium oxide formation

XRD analyses of ZrN and HfN test coupons after molten salt immersion experiments did not identify the formation of any reaction products on the sample surfaces. However, XRD pattern of the reaction products from a separate experiment, in which ZrN powder was reacted with LiCl-KCl-NaCl-UCl_3, confirmed the presence of UO_2 (Fig. 9). The UCl_3 component in the salt mixture was oxidized to UO_2. Among the salt mixture components UCl_3 is the least stable component and susceptible for conversion to an oxide. Table 2

shows that this oxidation reaction is thermodynamically spontaneous in the range of temperatures of interest. The source of oxygen for this reaction can be from a combination of the following sources: (a) residual oxygen impurities in the argon gas, which was measured to be in the parts per million ranges and (b) oxygen dissolved in the salt and test coupons prior to reaction. As shown in Table 2, oxidation of UCl_3 releases gaseous chlorine. This chlorine could react with ZrN or HfN to form $ZrCl_4$ and $HfCl_4$ volatile compounds, respectively making identification of condensed phases on the material surfaces or in the salts impossible. Although neither formation of $ZrCl_4$ or $HfCl_4$ was confirmed by analyzing the downstream gas, a white smoke was observed during the reaction above 500°C. This white smoke gets condensed at the scrubber end of the downstream gas line. EDS analysis on the condensed white powders indicated the presence of Zr, Hf and chlorine species. Extent of volatile compound formation increases with reaction time, and correspondingly more weight loss is observed (Fig. 4). Thus, formation of $ZrCl_4$ and $HfCl_4$ via oxidation of UCl_3 explains the increase in weight loss with reaction time observed at 525 (for all reaction times) and 700°C (up to 96 hours). But this does not explain the decrease in weight loss observed at 700°C at 96 hours (Fig. 4) and for all reaction times at 900°C compared to 525°C (Fig. 5). Thus, at higher reaction temperatures the dominant reaction mechanism is believed to be different than at 525°C as discussed in the next section.

4.3 Surface oxidation of test coupons

Semi-quantitative EDS analysis indicates that the oxygen enriched layers in ZrN and HfN could be solid solutions of Zr-N-O or Hf-N-O (oxynitrides). As seen in Table 1, as the temperature increased from 525 to 900°C the thickness of the oxygen enriched layer increased; and correspondingly the weight loss and Zr ion concentration present in the salt solution decreased. From the results presented in Table 1, it is proposed that as temperature increases, an oxygen rich surface layer forms and protects the test coupons, namely the ZrN and HfN from the chlorination process or electrochemical dissolution (Table 2). This results in a decrease in the amount of weight loss. In a study by Ikuma and Shoji [16] on the high temperature oxidation of ZrN powder, the authors reported that the onset of oxidation was observed at 680°C, and the powders turned black in color. In our present study, surfaces of nitrides tested at 700°C and 900°C appeared black in color. The presence of an oxide on the surface was not confirmed during post-test characterization. However, as reported earlier, an oxygen-enriched layer, likely an oxynitride phase [9, 12], was observed. Therefore, at 700 and 900°C the dominant reaction likely changes due in part to the formation of a surface oxide or oxynitride. The change in the surface composition could restrict electrochemical dissolution and/or chlorination reaction at 700 and 900°C.

4.4 Volatile product formation/electrochemical dissolution and surface oxidation

At 525°C, formation of volatile products (via chlorination reaction) and or electrochemical dissolution seems to dominate over the formation of an oxynitride phase (Table 1). This observation can be made from the following results: (a) relatively higher weight loss of ZrN and HfN at 525°C than 700 and 900°C (b) relatively higher Zr ion concentration present in the salt solution studied at 525°C (Table 1) and (c) increase in weight loss. In addition, the surfaces of nitrides tested at 525°C exhibited a golden color indicative of pure ZrN and HfN. But the surface turned black in color when tested at 700 and 900°C, signifying a surface oxidation reaction had occurred. Thus, at high temperature regimes (700 and 900°C) formation of oxynitride phase dominates over electrochemical dissolution as evidenced by the relative increase in the thickness of the oxynitride layer, decrease in the Zr ion concentration, and decrease in the weight loss values of ZrN and HfN tested at 700 and 900°C.

4.5 Apparent activation energy

Calculation of apparent activation energy of processes that occur by the simultaneous operation of different mechanisms is well documented in the literature [17-20]. In this study of molten salt reactions of ZrN and HfN, evidence indicates the simultaneous occurrence of different mechanisms such as electrochemical dissolution/formation of volatile products and/or oxynitride formation. In similar cases of competing reactions, negative activation energy was reported in the literature [18-20]. Fig. 11 shows the Arrhenius plot between natural logarithm of rate and inverse temperature for weight loss data at 96 hours. The recession rate (μm/s) was calculated by normalizing the weight loss data with reaction time and theoretical density of ZrN and HfN. A linear kinetic process was assumed in the calculation of activation energy. As observed in the

literature [18-20], a negative apparent activation energy value of -46 k J/mol and -28 k J/mol [Fig. 11] was observed for the molten salt reaction of ZrN and HfN, respectively. This seemingly anomalous negative activation energy can be physically construed as the manifestation of two or more fundamental mechanisms responsible for the weight loss.

4.6 Phenomenological model

Fig. 12 shows a schematic representation of a phenomenological model for reactions of ZrN in LiCl-KCl-NaCl-UCl_3 solution. The proposed model can be explained as follows:

(i) At 525°C ZrN dissolves electrochemically in the molten salt solution. Electrochemical dissolution is schematically represented in Fig. 12 by the removal of Zr^{4+} ions from ZrN surface. The dissolution resulted in weight loss of the bulk sample. The absence of an oxynitride phase at 525°C left the nitride surface unprotected and exposed completely to the molten salt solution.

(ii) In addition to dissolution, ZrN could react with $Cl_2(g)$ or Cl^- ion to form $ZrCl_4$ and $N_2(g)$. In Fig. 12, the arrows representing the diffusion of $ZrCl_4$ and $N_2(g)$ from the ZrN surface depict this reaction. The primary source of $Cl_2(g)$ is suggested to be from the oxidation reaction of $UCl_3(s)$ to $UO_2(s)$ and $Cl_2(g)$. Key evidence for this observation is from the XRD pattern given in Fig. 9.

(iii) At 700 and 900°C, ZrN formed an oxynitride layer at the surface. The thickness of the oxynitride phase increased with increased reaction time and temperature. For example, the thickness of the oxynitride phase in ZrN after 96 hours was 30 and 70 µm at 525 and 700°C, respectively. The source of oxygen could be diffusion of oxygen to the surface from ZrN itself since hot pressed ZrN was found to have dissolved oxygen impurities. However, further studies have to be done to confirm the source of oxygen.

(iv) The oxynitride layer appears to inhibit dissolution and penetration of $Cl_2(g)$ and chlorine ions. Thus, formation of oxynitride at 700 and 900°C controls the weight loss. Further study is required to evaluate the specific rate limiting mechanisms.

5. Conclusions

The durability of ZrN and HfN was evaluated in molten 28.5 % LiCl- 36.3 % KCl-29.4 % NaCl- 5.8 % UCl_3 (in weight percent) at temperatures ranging from 525 to 900ºC for reaction times of 4 to 485 hours under argon atmosphere. ZrN and HfN experienced weight loss under all experimental conditions. However, weight loss decreased with an increase in temperature, and the highest weight loss values were observed in immersion experiments done at 525ºC. Experimental evidence indicates that weight loss is due to formation of volatile products and or electrochemical dissolution.

Formation of Zr-Cl and Hf-Cl volatile products is believed to occur due to reaction of the nitrides with $Cl_2(g)$ or Cl^-, which could be generated due to reaction of UCl_3 species present in the salt with oxygen. The source of oxygen for this reaction could have come from oxygen residual impurities in argon gas, test coupons, and/or salt. However the source needs to be confirmed by further analysis. Occurrence of the reaction was confirmed by the presence of a UO_2 phase in the XRD analysis of the salt species after immersion testing. It is, thus, concluded that during electrorefining and cathode processing, a low p_{O_2} value in the processing atmosphere may reduce the crucible damage. Occurrence of electrochemical deposition is believed to be occurring from the observed presence of Zr ion concentration (through ICP-MS analysis) in the salt species after immersion testing.

At 700 and 900ºC, the formation of oxynitride phase at the surface seems to prevent the formation of volatile product and electrochemical dissolution. Thus the simultaneous occurrence and competition of electrochemical dissolution and oxidation resulted in negative activation energy values.

Acknowledgements

The authors would like to thank Gordon Balfour at Boise State University for help with the experimental setup. Special thanks to Franklin Bailey, Dr. Thomas Williams and Dr. Batric Pesic at University of Idaho for allowing to use their SEM; Charles Knaack at Geological laboratory, Washington State University for his help in ICP-MS; and Darin Ray at Ceramatec Inc., for his help in hot-pressing of the nitrides. The primary author [PP] gratefully acknowledges Boise State University, which provided him with a Graduate Residential Scholars Fellowship. This work was supported by Idaho National Laboratory, the Department of Energy, and the Center for Advanced Energy Studies.

References

[1] J. J. Laidler, J. E. Battles, W. E. Miller, J. P. Ackerman and E. L. Carls, Development of Pyroprocessing Technology, Prog. Nucl. Energy, 31 (1997) 131-140.

[2] T. Ogawa, K. Minato, Dissolution and Formation of Nuclear Materials in Molten Media, Pure Appl. Chem., 73 (2001) 799-806.

[3] F. Kobayashi, R. Ogawa, M. Akabori, Y. Kato, Anodic dissolution of uranium mononitrides in lithium chloride-potassium chloride eutectic melt, J. Am. Ceram. Soc., 78 (1995) 2279-2281.

[4] O. Shirai, T. Iwai, K. Shiozawa, Y. Suzuki, Y. Sakamura, T. Inoue, Electrolysis of plutonium nitride in LiCl-KCl eutectic melts, J. Nucl. Mater., 277 (2000) 226-230.

[5] T. Usami, M. Kurata, T. Inoue, H. E. Sims, S. A. Beetham, J. A. Jenkins, Pyrochemical reduction of uranium dioxide and plutonium dioxide by lithium metal, J. Nucl. Mater., 300 (2002) 15-26.

[6] B. R. Westphal, J. C. Price, D. Vaden, R. W. Benedict, Engineering-Scale Distillation of Cadmium for Actinide Recovery, J. Alloys Compd., 444-445 (2007) 561-564.

[7] M. Takeuchi, T. Kato, K. Hanada, T. Koizumi and S. Aose, Corrosion Resistance of Ceramic Materials in Pyrochemical Reprocessing Condition by Using Molten Salt for Spent Nuclear Oxide Fuel, J. Phys. Chem. Solids, 66 (2005) 521-525.

[8] A. Ravi Shankar, U.K. Mudali, R.Sole, H.S. Khatak, B.Raj, Plasma-sprayed yttria-stabilized zirconia coatings on type 316L stainless steel for pyrochemical reprocessing plan, J. Nucl. Mater., 372 (2008) 226-232.

[9] D. I. Bazhanov, A. A. Knizhnik, A. A. Safonov, A. A. Bagatur'yants, M. W. Stoker, A. A. Korkin, "Structure and Electronic Properties of Zirconium and Hafnium Nitrides and Oxynitrides", J. Appl. Phys., 97 (2005) 044108-1-044108-6.

[10] A. K. Santhanam, Application of Transition Metal Carbides and Nitrides in Industrial Tools, in: S. Ted Oyama (Ed.), The Chemistry of Transition Metal Carbides and Nitrides, Chapman & Hall, Great Britain, 1996, pp. 28-52.

[11] P. Periasamy, Compatibility Assessment of HfN, ZrN and Graphite with Molten LiCl- NaCl- KCl-UCl_3, MS thesis, Boise State University, Boise, 2008.

[12] W.Q.Zhang, L.Y.Huang, A.D.Li, Q.Y.Shao, D.Wu, Chemical Vapor Deposition of $Zr_XHf_{1-X}O_2$ Thin Films Using Anhydrous Mixed-Metal Nitrate Precursors, Integrated Ferroelectrics, 97 (2008) 93-102.

[13] N. S. Jacobson, Kinetics and Mechanism of Corrosion of SiC by Molten Salts, J. Am. Ceram.

Soc., 69 (1986) 74-82.

[14] M. Fritsch, H. Klemm, M. Herrmann, B. Schenk, Corrosion of Selected Ceramic Materials in Hot Gas Environment, J. Eur. Ceram. Soc., 26 (2006) 3557-3565.

[15] S. Bourg, F. Peron, J. Lacquement, The Evaluation of the Pyrochemistry for the Treatment of Gen IV Nuclear Fuels – Inert Matrix Chlorination Studies in the Gas Phase or Molten Chloride Salts, J. Nucl. Mater., 360 (2007) 58-63.

[16] Y. Ikuma and A. Shoji, High Temperature Oxidation of ZrN Powder in Oxygen Atmosphere, in: N.Mizutani (Ed.), Advanced Materials '93, I / A: Ceramics, Powders, Corrosion and Advanced Processing, Transactions of Materials Research Society of Japan, Volume 14A, Elsevier, Amsterdam, 1994, pp. 277-280.

[17] J. F. Nicholas, Apparent Activation Energy and Frequency Factor for a Process Involving Competing Mechanisms, J. Chem. Phys., 31 (1959) 922-925.

[18] J. Wei, Adsorption and Cracking of N-Alkanes Over ZSM-5: Negative Activation Energy of Reaction, Chem. Eng. Sci., 51 (1996) 2995-2999.

[19] K. N. Houx, N. G. Rondan, J. Mareda, Theoretical Studies of Halocarbene Cycloaddition Selectivities, Tetrahedron, 41 (1985) 1555 – 1563.

[20] M. Bettman, N. C. Otto, A case of Negative Apparent Activation Energy Due to Pore Diffusion Effects, Chem. Eng. Sci., 38 (1983) 491-493.

Table 1
The effect of reaction conditions on (a) weight loss of ZrN (b) thickness of the oxygen enriched layer in ZrN, and (c) Zr ion concentration in the salt after immersion experiment. The salt composition was 28.5% LiCl- 36.3% KCl-29.4% NaCl- 5.8% UCl_3 (in weight percent). The p_{O_2} value was maintained below 1 ppm (by volume) during the immersion experiment. N/A indicates data unavailable.

Reaction conditions	Weight loss (mg/cm^2)	Thickness of the oxygen enriched layer (μm)	Zr ion concentration in the salt after immersion experiment (appm)
525°C for 96 hours	-13.62	30	204
700°C for 96 hours	-9.49	50	82.1
900°C for 96 hours	-2.86	70	N/A

Table 2
Free energy (ΔG) values of oxidation of UCl_3 and chlorination of ZrN and HfN at 525 and 700°C. Calculations were done with HSC Outokompu software.

Equation	ΔG at 525°C (kJ)	ΔG at 700°C (kJ)
$UCl_3 + O_2(g) = UO_2 + 3/2\ Cl_2(g)$	-258.2	-264.7
$ZrN + 2Cl_2(g) = ZrCl_4 + 1/2\ N_2(g)$	-454.8	-423.2
$HfN + 2Cl_2(g) = HfCl_4 + 1/2\ N_2(g)$	-464.7	-433.2

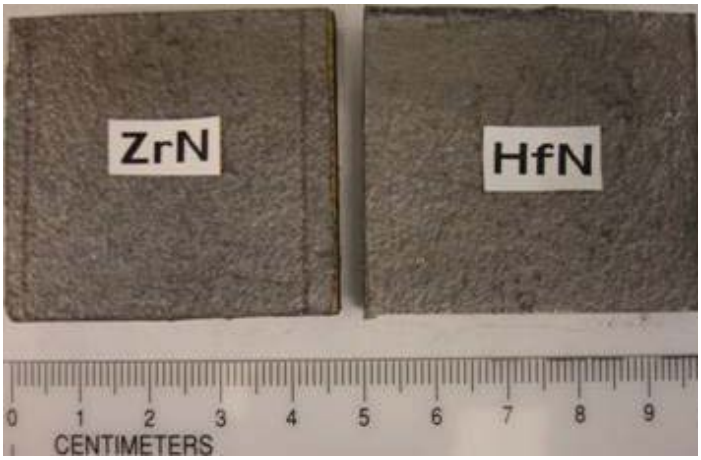

Fig. 1. Photograph of hot pressed ZrN and HfN plates

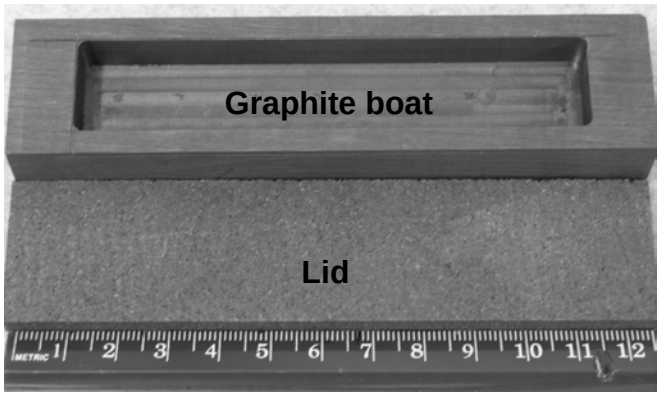

Fig. 2. Photograph of a graphite boat and lid employed in molten salt immersion test.

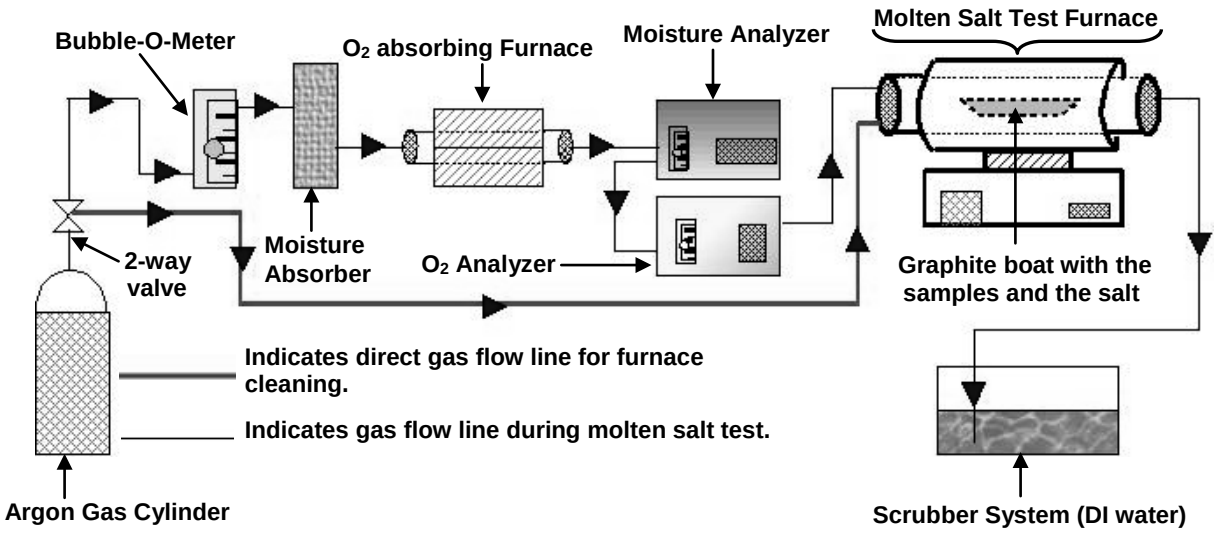

Fig. 3. Schematic representation of the molten salt test setup. During the molten salt immersion test, argon gas flows through the moisture and O_2 absorber before flowing through the molten salt test furnace. The p_{O_2} value is maintained below 1 ppm (by volume) for all the immersion experiments in this study.

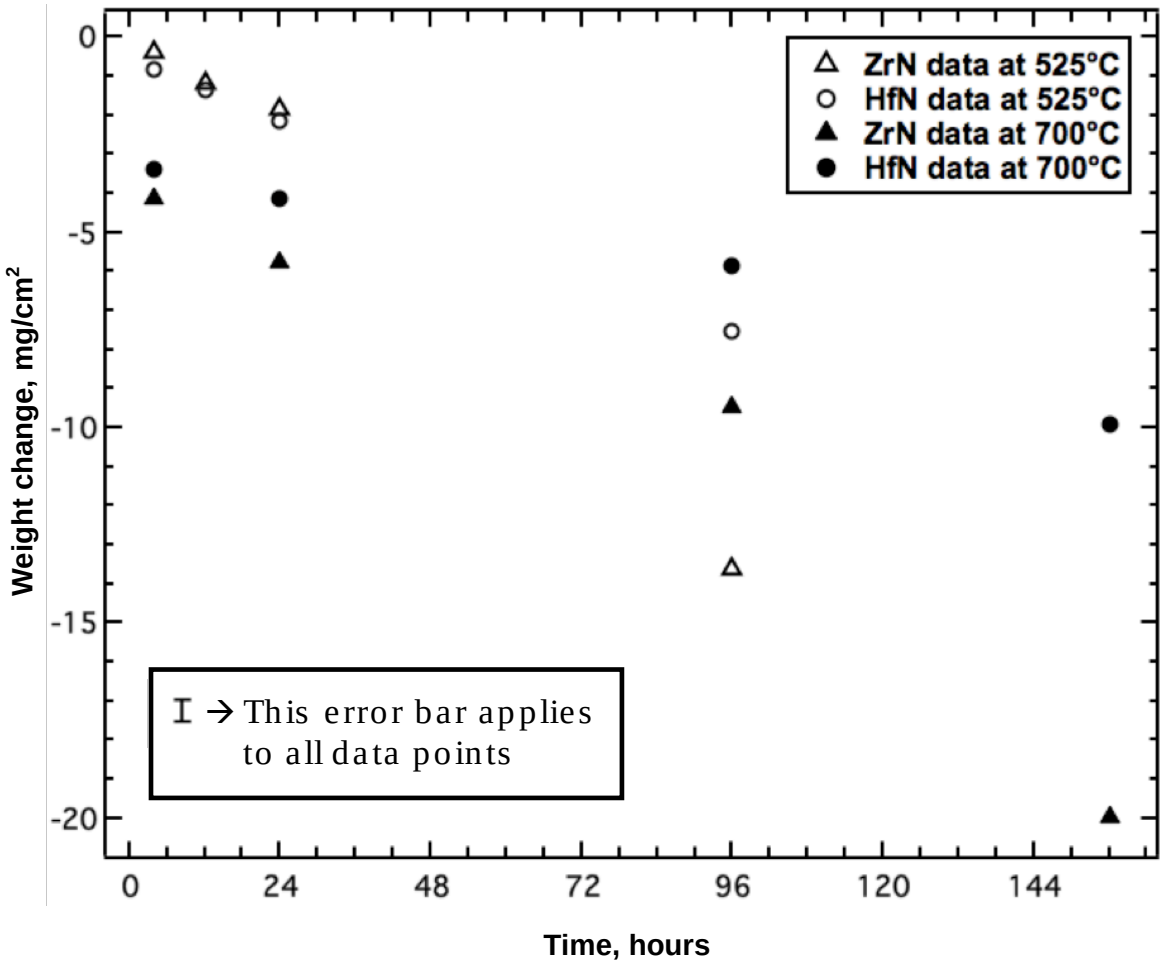

Fig. 4. Reaction kinetics of ZrN and HfN exposed to 28.5 % LiCl- 36.3 % KCl- 29.4 % NaCl- 5.8 % UCl_3 (in weight percent) at 525 and 700°C as a function of time. The p_{O_2} value is less than 1 ppm (by volume). Error bar indicates the standard deviation associated with the dimension and weight measurements. Data points at 12 and 96 hours are repeated twice and found to be consistent.

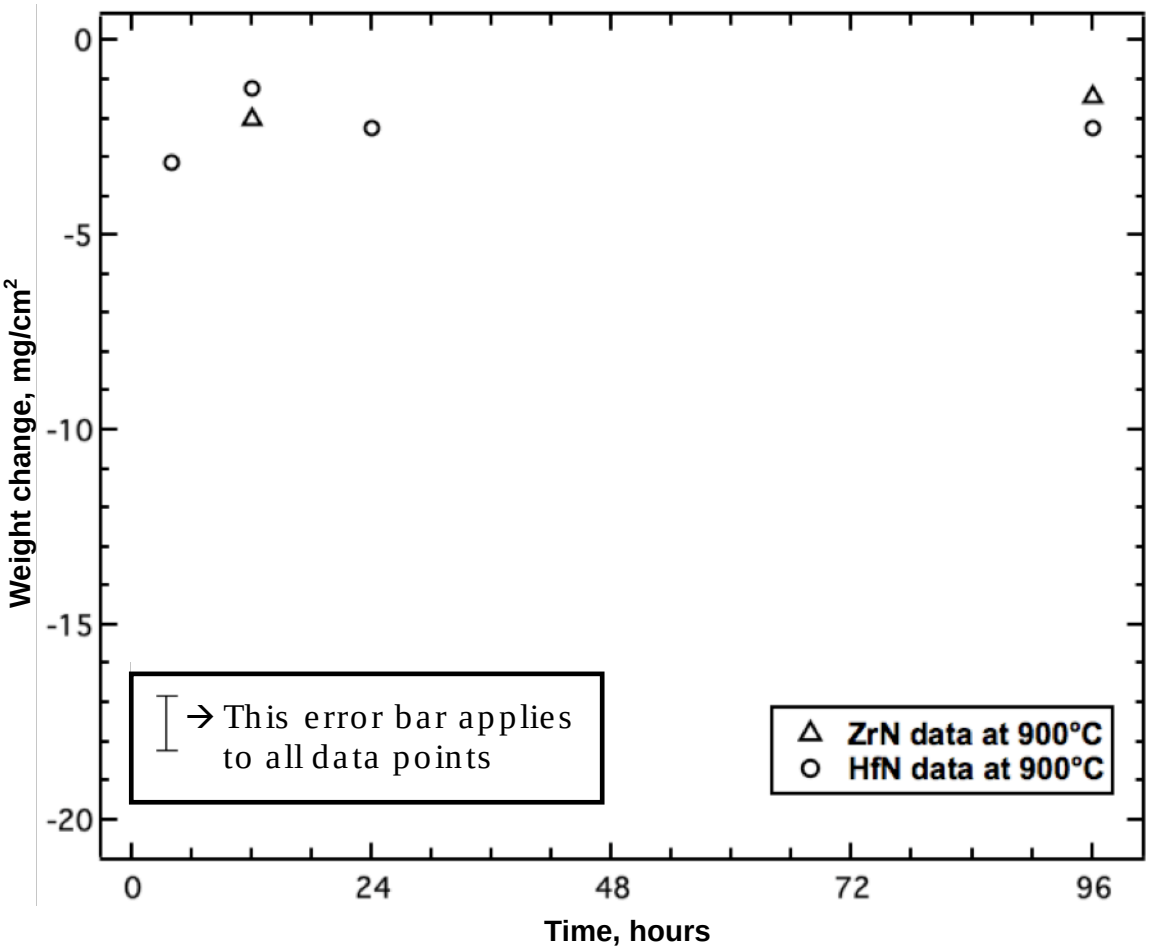

Fig. 5. Bar chart showing reaction kinetics of ZrN and HfN in 28.5 % LiCl- 36.3 % KCl-29.4 % NaCl- 5.8 % UCl_3 (in weight percent) at 900°C as a function of time (4, 12, 24 and 96 hours). The p_{O_2} value is less than 1 ppm (by volume). A reliable data could not be recorded for ZrN at 4 and 24 hours. Error bar indicates the standard deviation associated with the dimension and weight measurements.

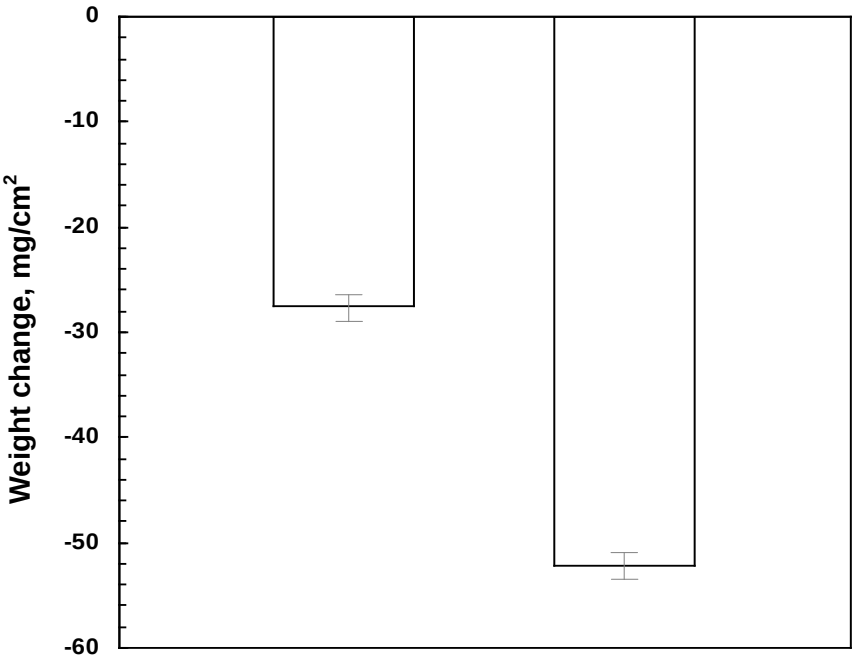

Fig. 6. Bar chart showing weight loss of ZrN and HfN in 28.5 % LiCl- 36.3 % KCl-29.4 % NaCl- 5.8 % UCl_3 (in weight percent) at 585°C for 485 hours (the longest corrosion time in this study). The p_{O_2} value is less than 1 ppm (by volume). Error bars indicate the standard deviation associated with the dimension and weight measurements.

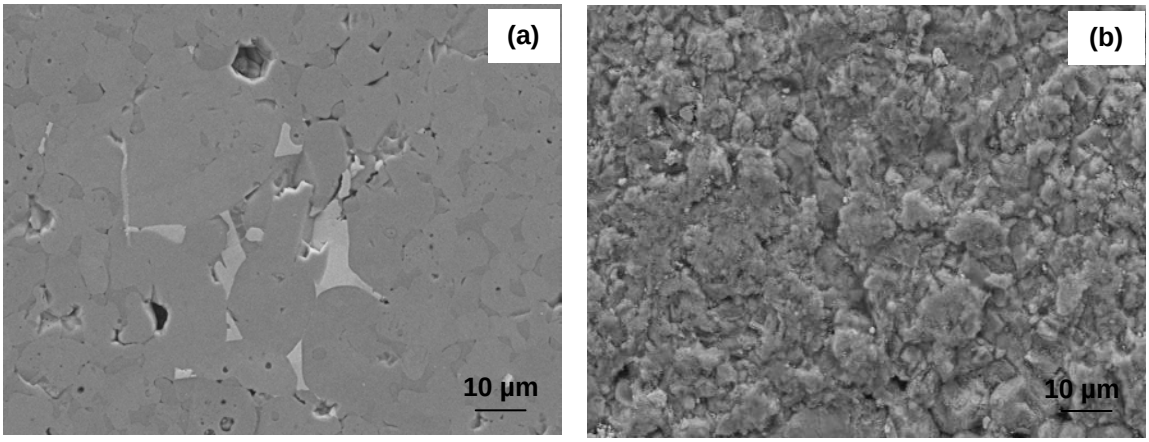

Fig. 7. SEM micrograph showing (a) a polished surface of the as- hot pressed ZrN and (b) cleaned surface after exposure to 28.5 % LiCl- 36.3 % KCl-29.4 % NaCl- 5.8 % UCl_3 (in weight percent) at 525ºC (p_{O_2} less than 1 ppm by volume) for 96 hours.

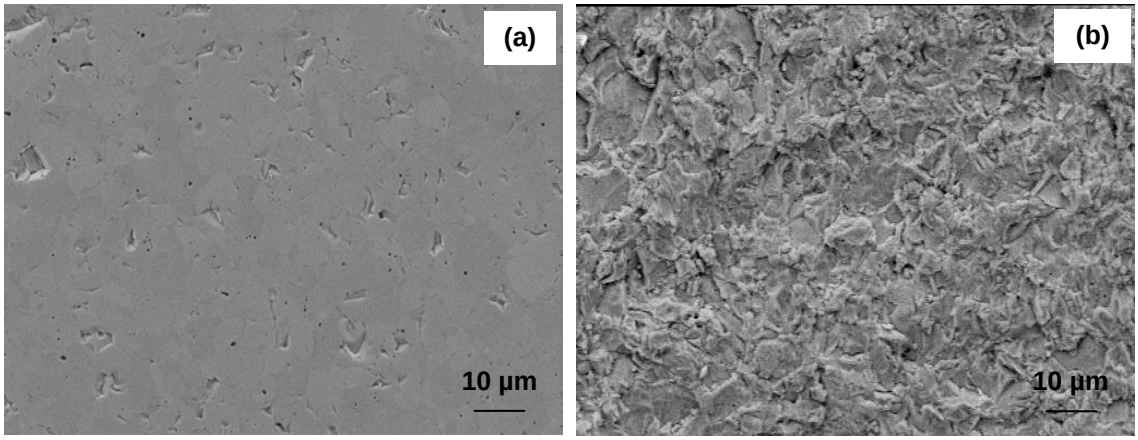

Fig. 8. SEM micrographs showing (a) a polished surface of as-hot pressed HfN and (b) cleaned surface after exposure to 28.5 % LiCl- 36.3 % KCl-29.4 % NaCl- 5.8 % UCl_3 (in weight percent) at 525ºC (p_{O_2} less than 1 ppm by volume) for 96 hours.

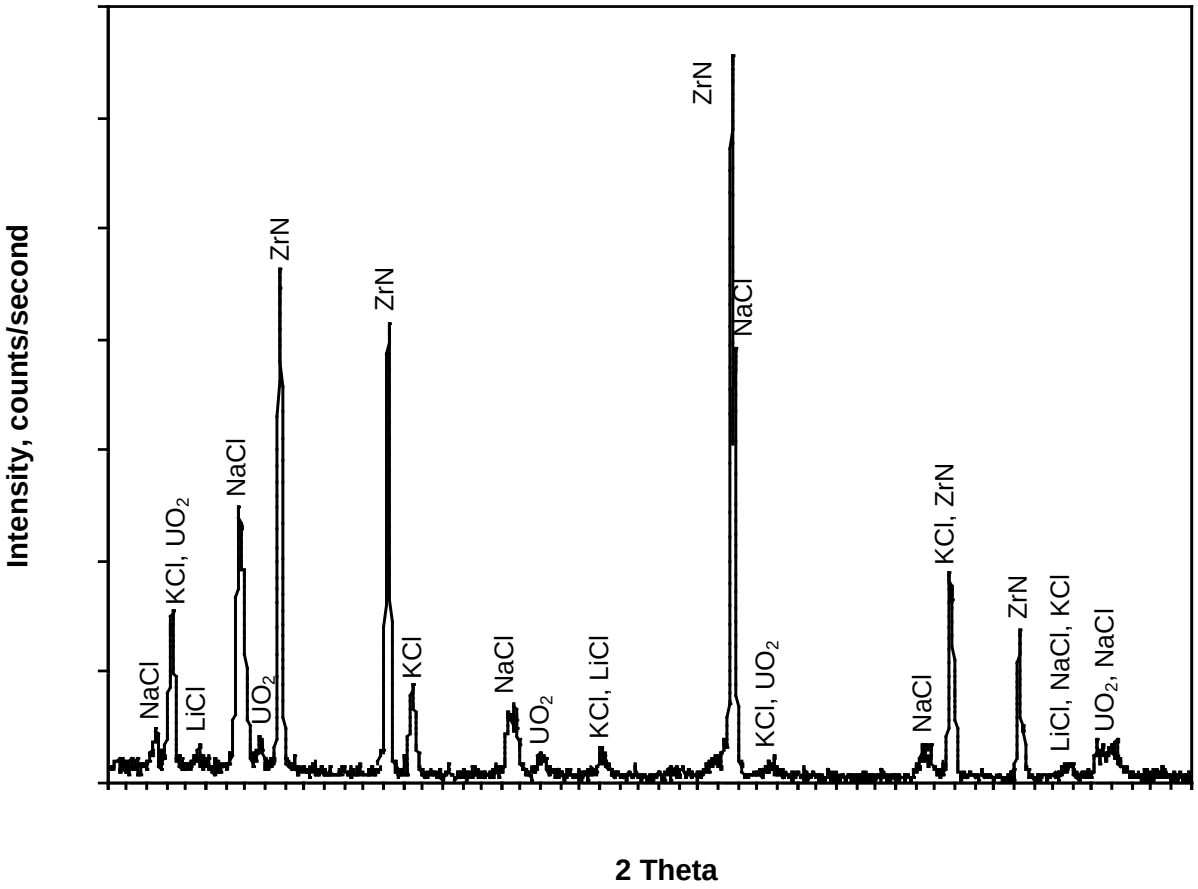

Fig. 9. XRD pattern of mixture of ZrN powder and 28.5 % LiCl- 36.3 % KCl- 29.4 % NaCl- 5.8 % UCl_3 (in weight percent) after molten salt tested at 900°C (p_{O_2} less than 1 ppm by volume) for 1 hour

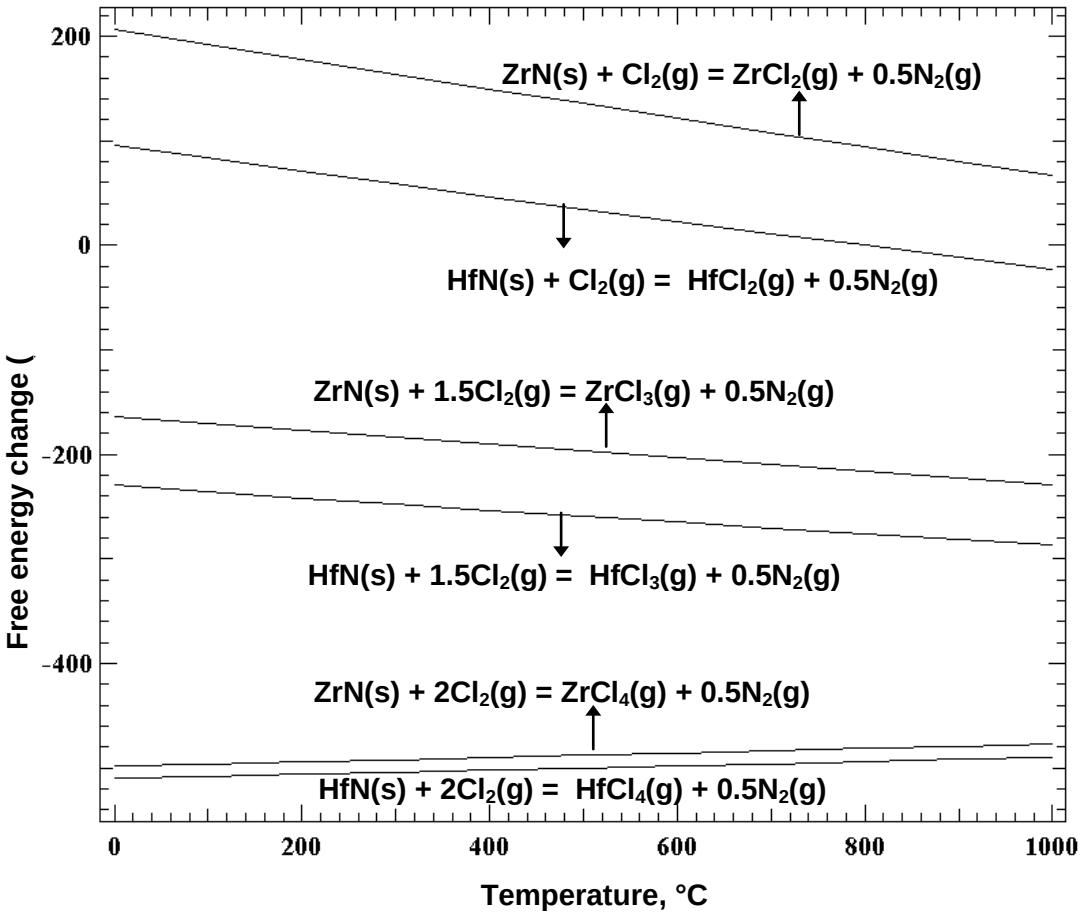

Fig. 10. Free energy change of Zr-Cl and Hf-Cl compounds. In Zr-Cl compounds, $ZrCl_4$, $ZrCl_3$ and $ZrCl_2$ gaseous phases are plotted. In Hf-Cl compounds, $HfCl_4$, $HfCl_3$ and $HfCl_2$ gaseous phases are plotted. Energy calculations were performed using HSC Outokompu software.

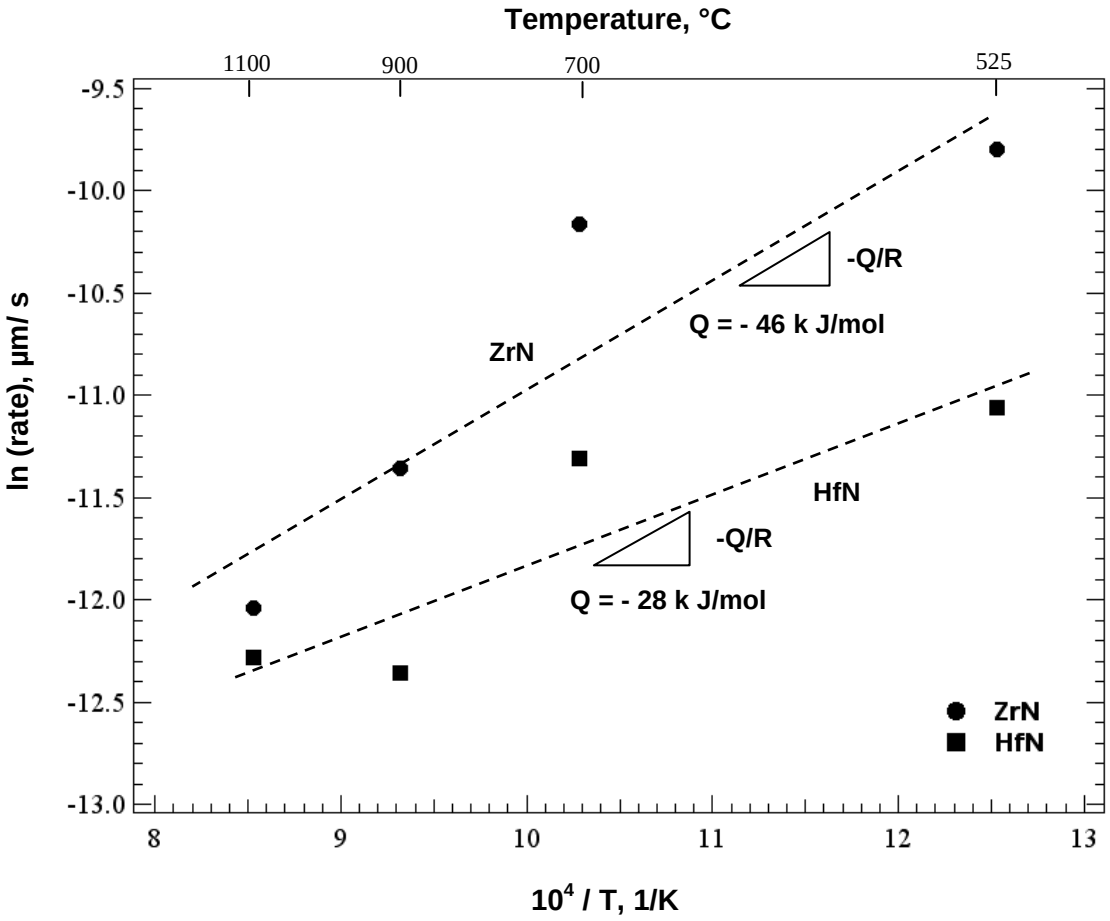

Fig. 11. Arrhenius plot between natural logarithm of rate and inverse temperature of ZrN and HfN exposed to 28.5 % LiCl- 36.3 % KCl-29.4 % NaCl- 5.8 % UCl_3 (in weight percent) at 96 hours. Dotted line represents the linear fit. Q represents the calculated anomalous, apparent activation energy.

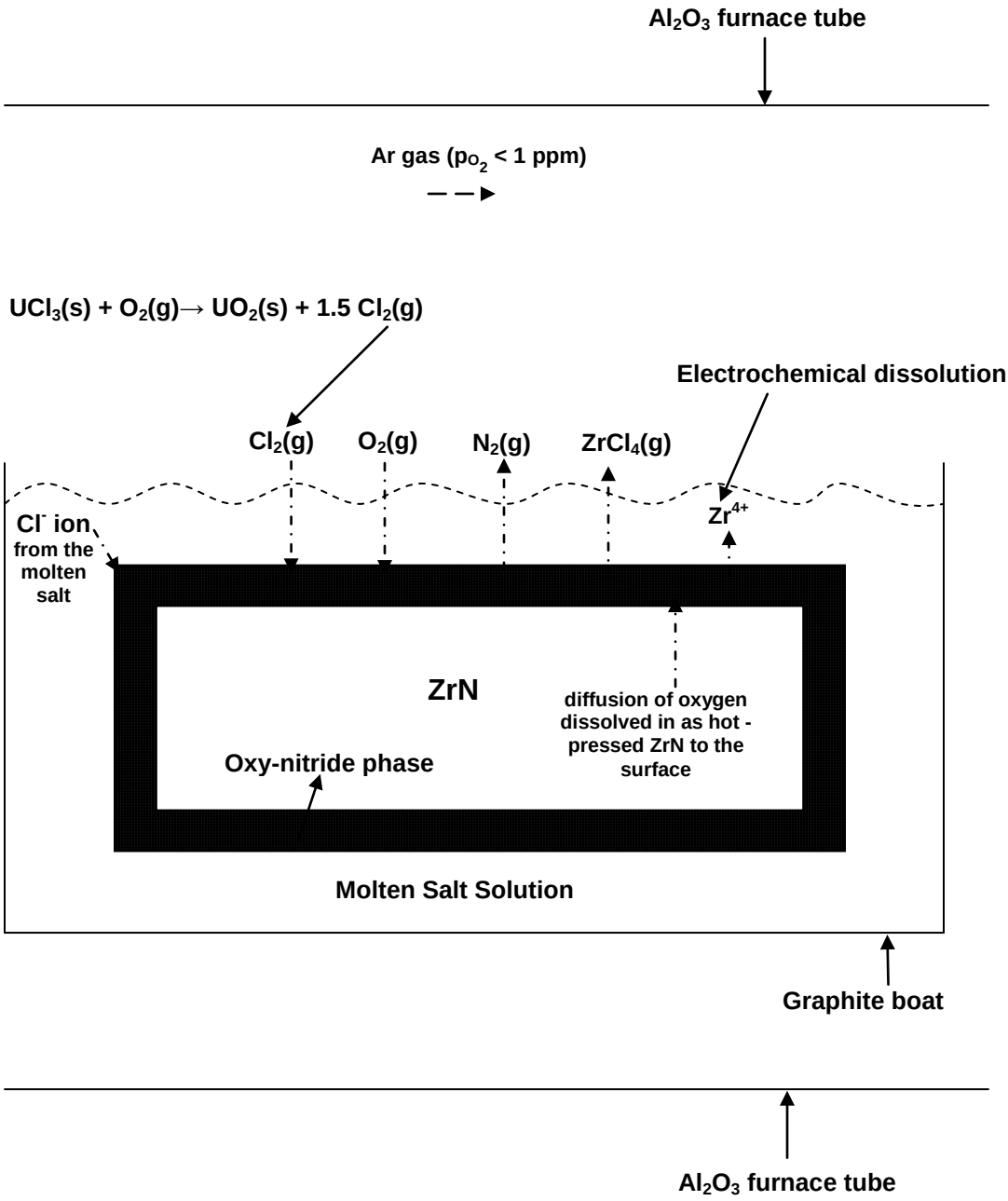

Fig. 12. Schematic representation of possible reaction processes involving ZrN in 28.5 % LiCl- 36.3 % KCl-29.4 % NaCl- 5.8 % UCl_3 (in weight percent).